JPSE (Journal of Physical Science and Engineering), Vol. 9, No. 1, 2024, Page 1–8.
DOI: 10.17977/um024v9i12024p001

JPSE
(Journal of Physical Science and Engineering)

http://journal2.um.ac.id/index.php/jpse
EISSN: 2541-2485

Integrated Slope Safety Factor Analysis Using Geotechnical Bishop Method and Resistivity Method for Calculating Landslides Probabilities in Imogiri area, Special Region of Yogyakarta

Received
1 January 2024

Revised
21 February 2024

Accepted for Publication
19 Maret 2024

Published
30 Maret 2024

Burhanuddin Fahmi and Y. Yatini *

Geophysics Engineering, UPN Veteran Yogyakarta, Jalan SWK 104 (North RingRoad), Condongcatur, Yogyakarta 55283, Indonesia.

***E-mail:** jeng_tini@upnyk.ac.id

Abstract

Landslides potential analysis is very serious issue in disaster mitigation processes. The risk of landslide potential in a slope can be assessed through the calculation of Slope Safety Factors, involving data on soil physical properties, soil mechanics (geotechnical properties), and slope geometry. Research was conducted using a combination of resistivity and Bishop geotechnical methods. The geoelectric method was employed to determine the lithology of landslide materials and the geometry of the sliding plane. The Bishop geotechnical method was used to calculate the slope safety factor based on geoelectric data, soil mechanics data, and rock mechanics data obtained in the study area. A total of 9 geoelectric measurement profiles, each 120-150 meters long, were taken in the Imogiri region of Yogyakarta. The research results indicate that the sliding plane is located at a depth of 10 meters with clay lithology. The calculated slope safety factor using the Bishop method was performed under two conditions: saturated and unsaturated. The saturated slope safety factor has a low value, less than 1.07, while the unsaturated condition yields a higher value, greater than 1.25.

Keywords: Landslide, Geophysics, Geotechnical, Bishop, Safety Factor.

1. Introduction

Among the numerous natural hazards, landslides are one of the greatest, as they can cause enormous loss of life and property, and affect the natural ecosystem and their services. Landslides are disasters that cause damage to anthropic activities and innumerable loss of human life, globally [1]. The Geological Agency of the Ministry of Energy and Mineral Resources recorded that throughout the year 2020, Indonesia experienced 2,099 landslide incidents resulting in 304 fatalities, 7,266 displaced individuals, and 6,310 damaged houses (ESDM). Active tectonic plates in the Indonesian archipelago, including the Eurasian Plate, Indo-Australian Plate, and Pacific Plate, contribute to Indonesia's extensive mountainous terrain. Additionally, Indonesia's geographical location near the equator results in a tropical climate with high rainfall intensity. Consequently, Indonesia is a country highly susceptible to landslide disasters [2].

The risk of potential landslides on a slope can be assessed through the calculation of Slope Safety Factors, involving data on soil physical properties, soil mechanics (geotechnical properties), and slope geometry [3]. Specifically, the analysis can be further refined by considering other physical aspects regionally, such as environmental conditions related to seismic activity, climate, vegetation, morphology, rock/soil types, and local situations. Geophysical methods are employed to determine the lithology of the slope constituents and the geometry of the sliding plane. Geotechnical methods, including mechanical properties and physical characteristics of the soil, along with Bishop stability analysis, are used to determine the slope safety factor [4].

The research area falls within the Pegunungan Selatan Zone, which is divided into three subzones: Baturagung Subzone, Wonosari Subzone, and Gunung Sewu Subzone. Generally, the

Pegunungan Selatan Zone constitutes an uplifted and southward-tilted block with a maximum width of 55 kilometers to the south of Surakarta [6]. The Semilir Formation consists of volcanic rocks resulting from acidic volcanic eruptions. It is predominantly composed of lapilli tuff and tuff, with localized mixing of clastic sediments in the lower part. The lower section of this formation is dominated by lapilli tuff with interbedded tuff and clay tuff, as well as tuffaceous sandstone and brecciated volcanic rock. The upper part of the formation is primarily composed of tuff with interbedded lapilli tuff, tuffaceous sandstone, and sandstone conglomerate [7].

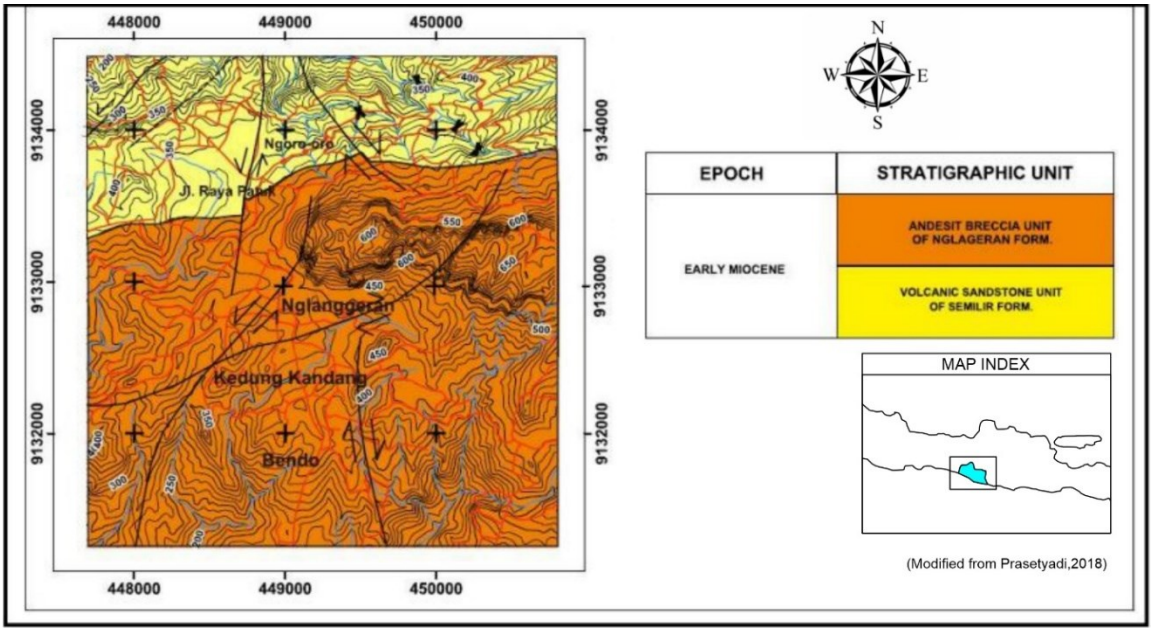

Figure 1. Geological Map in the research area[5].

The Semilir Formation overlies the Kebo-Butak Formation in a conformity, it consists of volcanic rocks resulting from acidic volcanic eruptions. The dominant lithologies include lapilli tuff and tuff, with localized mixing of clastic sediments in the lower part. Specifically, the lower section of this formation is characterized by lapilli tuff with interbedded tuff and clay tuff, as well as tuffaceous sandstone and brecciated volcanic rock. In the upper part of the formation, tuff is the prevailing rock type, along with interbedded lapilli tuff, tuffaceous sandstone, and sandstone conglomerate. The Semilir Formation is estimated to be 20 to 16 million years old (Early Miocene). Generally, the lower part of the Semilir Formation was deposited in a marine environment, which later transitioned to terrestrial conditions during the deposition of the upper Semilir Formation. The combined thickness of both the lower and upper Semilir Formations is approximately 460 meters [7].

The Nglanggran Formation is predominantly composed of lithologies such as breccia, volcanic sandstone, and tuff interbeds in its lower section. As we move to the upper part of the Nglanggran Formation, it is characterized by volcanic sandstone, sandstone breccia, and brecciated rocks [8]. Petrographic observations reveal that the volcanic rocks of the Nglanggran Formation are primarily composed of clay-dominated mineralogy, resulting in highly compacted and low-porosity rock. The breccia found within the Nglanggran Formation consists of sediment fragments that are in close contact or interlocked with each other, preventing water retention within the rock [9]. The Nglanggran Formation overlies the Semilir Formation in a conformity and consists of units of volcanic breccia and agglomerate, with interbedded tuff and andesitic lava[7]. The Nglanggran Formation is located in Nglanggran Village, to the south of Semilir Village. It dates back to the Early Miocene period. The Nglanggran Formation has a thickness of approximately 530 meters, extending widely from the western part of Parangtritis to the eastern part of Gunung Panggung.

2. Method

2.1. Resistivity

Resistivity can be used to estimate of subsurface geological conditions by leveraging the electrical properties of rock in relation to the earth as a conductor [10]. Rock type and other parameters of the

earth's surface can be detected by injecting an electric current into the earth [11]. The Earth is assumed to be layered, with each layer having different resistivity values. The diversity in resistivity is influenced by various factors, including porosity, water content, and water quality [12]. Apparent resistivity refers to the resistivity of a hypothetical homogenous medium that is equivalent to a layered medium under consideration. For instance, when examining a layered medium composed of two layers with different resistivities (ρ_1 and ρ_2), it is treated as a single homogenous layer with an apparent resistivity value denoted as ρ_a [13].

$$\rho_a = K\frac{V}{I} \quad (1)$$

ρ_a : Apparent resistivity (Ωm)
V : Electric potential (mV)
I : Electric current (mA)
K : Configuration Factor

2.2. Dipole-dipole Configuration

The Dipole-Dipole geoelectric method generally shares the same fundamental principle with other configurations. It involves injecting current electrodes into the ground to measure the potential difference. The key difference lies in how the electrodes are arranged, which is adjusted based on field measurement conditions and the desired depth to determine the resistivity values beneath the Earth's surface [14]. The arrangement of current electrodes and potential electrodes with different positions leads to the use of varying geometric factors (k). The dipole-dipole method is commonly employed to observe subsurface conditions laterally, particularly for examining fault surfaces at shallow depths [12]. The Dipole-dipole configuration using configuration factor below.

$$k = \pi(n+1)(n+2)a \quad (2)$$

k : Configuration Factor
n : Sample multiplier

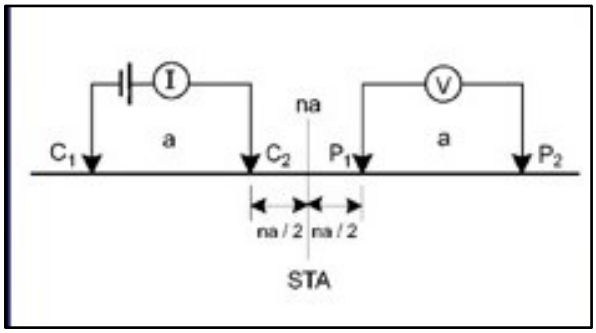

Figure 2. Dipole-Dipole configuration [15]

2.3. Bishop method

Slope stability analysis is employed to determine the safety factor of potential landslide areas. It relies on several assumptions, such as considering slope failure along a specific surface known as the slip plane or failure plane. One of the methods used for slope stability analysis is the Simplified Bishop Method, which simplifies the analysis process based on Bishop's original approach [16]. This method is the most popular approach in slope stability analysis.

$$SF = \frac{(\sum X/(1+YF))}{(\sum Z+Q)} \quad (3)$$

SF = Safety Factor
X = $(c' + (\gamma.\ h - \gamma w.hw)\tan\theta)\ \Delta x \cos\alpha$
Y = $\tan\alpha \tan\theta$
Z = $\gamma.\ h.\ \Delta x.\ \sin\alpha$
Q = 1 2 . γW. Z 2 (α R)
γ = Unit weight (ton/m3)

γw = saturated unit weight (ton/m3)
α = Slip plane slope (°)
θ = Shear angle (°)
h = Slope height (m)
hw = Saturated slope height (m)
c' = Cohession (Mp_a)
Z = Depth tensile stress (m)

The Bishop calculation method has been modified based on the Sweden arc calculation method while taking counterforce among splitting interfaces into consideration, which improves the precision of calculation results. The Simplified Bishop Method offers straightforward calculations, quick results, and provides slightly accurate safety factor calculations [17]. Using advanced analytical and numerical formulations, Bishop's method provides better modelling and a deeper understanding of slope stability mechanisms. Bishop method offers additional advantages over the Fellenius method in terms of taking a more accurate amount of the forces and moments of resistance mobilized in a slope [18].

A slope is a soil construction with varying elevations, resulting in gravitational forces that move the soil mass toward a lower surface. In determining slope stability, we encounter the concept of the Safety Factor, which represents the ratio between the resisting forces and the driving forces acting on the soil [19]. If the Safety Factor (SF) is greater than 1.25, the slope is generally considered stable. The stability of a slope is expressed by the Safety Factor, which represents the ratio between the resisting forces and the driving forces acting on the potential failure surface [20].

2. Result and Discussion

The inversion results of resistivity data in the research area exhibit a range of values, from a minimum of 1.28 Ωm to a maximum of 114 Ωm. Let's break down the classification based on these resistivity values very low resistivity includes resistivity values below 14 Ωm. The lithology associated with this very low classification consists of clay, which is found within the Semilir formation. Low Classification resistivity encompasses resistivity values ranging from 14 to 29 Ωm. In this range, the lithology corresponds to saturated sandstone tuff within the Semilir formation [21]. The intermediate classification corresponds to resistivity values ranging from 29 to 70 Ωm. In this range, the identified lithology consists of sandstone tuff within the Semilir formation. On the other hand, the high-class classification encompasses resistivity values exceeding 70 Ωm. The lithological interpretation for this high class involves breccia within the Nglanggran formation. The slip plane, characterized by its impermeability, hinders the passage of water. Consequently, water accumulates in the layer above it. In the research area, the slip plane is composed of clay, exhibiting a very low resistivity value of less than 14 Ωm [22]. The classification is presented in Table 1, along with the lithology and formations in the research area

Tabel 1. Resistivity Classification

No	Classification	Range of values ρ (Ωm)	Litology	Formation
1	Very Low	<14	Clay	Semilir
2	Low	14 – 29	Akuifer (Sandy Tuff)	Semilir
3	Medium	29 – 70	Sandy Tuff	Semilir
4	High	>70	Breccia	Nglanggran

2.1. Resistivity Interpretation

The slip plane is a non-permeable layer, making it difficult for water to pass through. Consequently, water accumulates in the layer above it. In the research area, the slip plane consists of clay, with a very low resistivity value of less than 14 Ωm at a depth of approximately 10 meters. An example can be found along track 1 (as shown in Figure 3), where the slip plane exhibits a geometry parallel to the slope, indicated by the dashed line in the figure. This alignment of the slip plane with the slope suggests a relatively high likelihood of landslides. The slip plane in the research area corresponds to clay within the Semilir formation, as depicted in Figure 2.

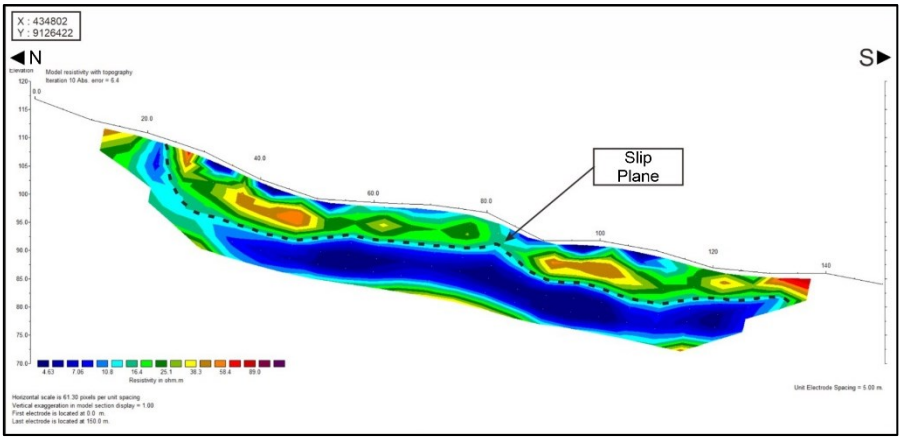

Figure 3. Resistivity Inversion Result of Track 1

The material composing the landslide lies above the slip plane and has a high porosity value. This high porosity allows the layer to retain a significant amount of water. Along track 1, the landslide material consists of soil and saturated sandstone tuff, exhibiting relatively high porosity. The resistivity of the sandstone tuff ranges from 29 to 70 Ωm at depths between 1 and 10 meters. This sandstone tuff lithology results from the deposition of volcanic activity within the Semilir formation.

Landslides can occur when lithologies with high porosity are directly above the slip plane. In the case of track 1, the presence of soil and sandstone tuff directly above the clay slip plane indicates a high risk of landslides. The geometry of the slip plane along track 1 aligns with the slope, causing the mass of landslide material above it to move relatively downward, resulting in a significant landslide hazard.

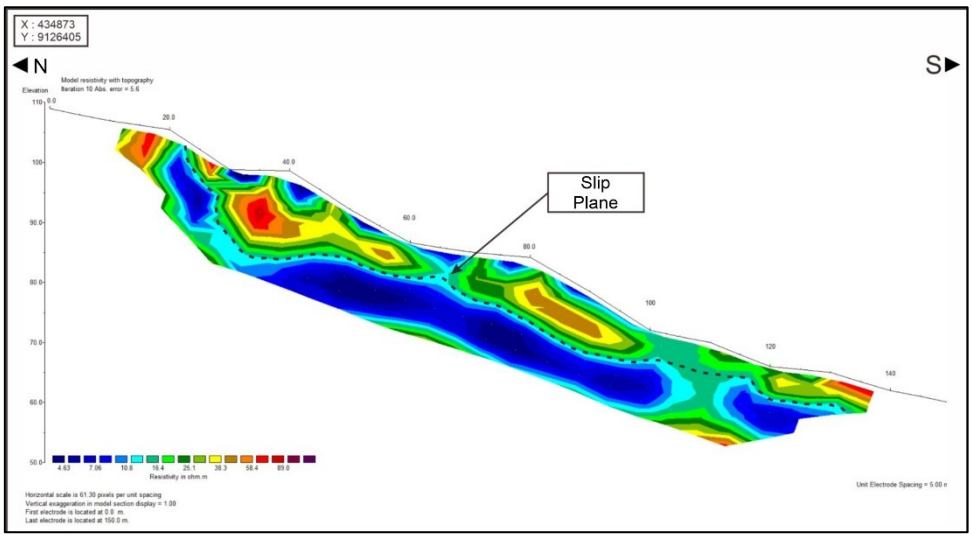

Figure 4. Resistivity Inversion Result of Track 2

The slip plane is a non-permeable layer, making it difficult for water to pass through. Consequently, water accumulates in the layer above it. In the research area, the slip plane consists of clay, with a very low resistivity value of less than 14 Ωm at a depth of approximately 10 meters. An example can be found along track 2 (as shown in Figure 4), where the slip plane exhibits a geometry parallel to the slope, indicated by the dashed line in the figure. This alignment of the slip plane with the slope suggests a relatively high likelihood of landslides. The slip plane in the research area corresponds to clay within the Semilir formation, as depicted in Figure 3.

The material composing the landslide lies above the slip plane and has a high porosity value. This high porosity allows the layer to retain a significant amount of water. Along track 1, the landslide material consists of soil and saturated sandstone tuff, exhibiting relatively high porosity. The resistivity of the sandstone tuff ranges from 29 to 70 Ωm at depths between 1 and 10 meters. This sandstone tuff

lithology results from the deposition of volcanic activity within the Semilir formation, specifically including other lithologies such as clay tuff, sandstone tuff, tuff lapilli, and breccia.

Landslides can occur when lithologies with high porosity are directly above the slip plane. In the case of track 2, soil and sandstone tuff directly above the clay slip plane indicates a high risk of landslides. The geometry of the slip plane along track 2 aligns with the slope, causing the mass of landslide material above it to move relatively downward, resulting in a significant landslide hazard.

2.2. Slope Safety Factor

The safety factor calculation in this research was performed using Rocscience Slide Version 6.0 software. The analysis of this safety factor is derived from processed shear strength test data, which includes cohesion values, internal friction angles, soil bulk density, and water content intensity within the soil. Landslides can be caused by several factors, including slope inclination, the lithology composing the slope, and the intensity of water present within the slope's lithology. These parameters are utilized to conduct a stability analysis of the slope, resulting in the determination of the Safety Factor as presented in Table 2 Slopes with high water intensity exhibit low safety factor values (<1.07).

Table 2. Safety Factor Classification [23]

No	SF Classification	SF Value	Safety Factor
1	Low	< 1,07	Unstble slope
2	Medium	1,07 – 1,25	Critical condition slope
3	High	> 1,25	Stable slope

A low safety factor indicates that the stability of the slope is poor or precarious. The safety factor is defined as the ratio between the resisting force and the force causing failure.

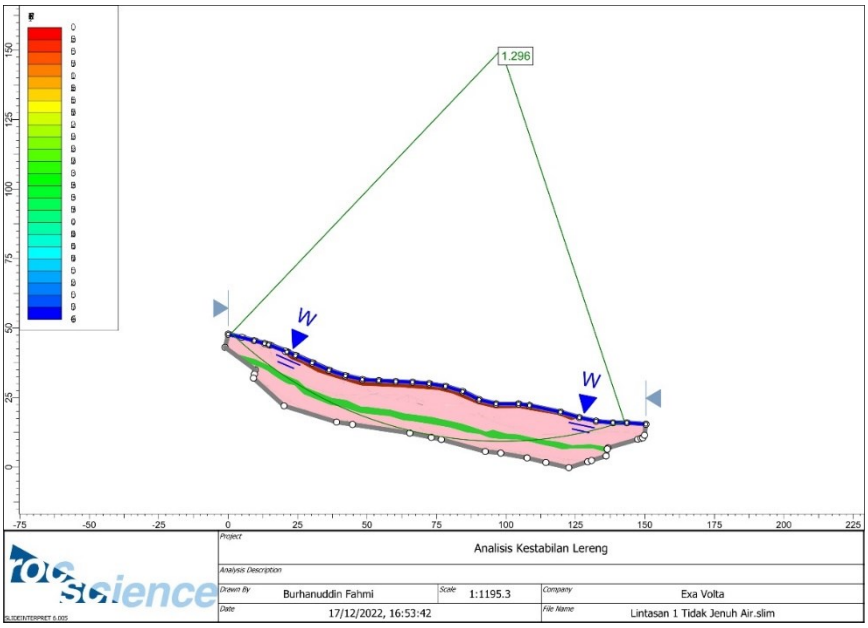

Figure 5. Line 1 Slope safety factor (non-water saturated)

The entire track indicates a slip plane parallel to the slope. The slip plane is found at depths ranging from 8 to 15 meters. The steep slope inclination combined with the slip plane's alignment parallel to the slope renders the slope critical or susceptible to landslides. In areas where the slope is unsaturated, there is no water retained within the landslide material. Unsaturated slopes have a lower likelihood of landslides due to the relatively low weight of the material.

For track 1, which is unsaturated, as shown in Figure 5, the calculated slope safety factor is 1.296. This value indicates an extremely low probability of landslides, consistent with the information in Table 2. Conversely, saturated slopes result from rainwater accumulation within the landslide material due to its favorable porosity. Saturated landslide material has a higher density, leading to

greater weight exerted on the slip plane. Saturated areas have a higher potential for landslides because the increased material weight significantly impacts slope stability.

3. Conclusion

The lithology present in the research area includes clay tuff, saturated sandstone tuff, and breccia. Here are their resistivity characteristics: Clay Tuff: Has a very low resistivity, less than 14 Ωm. Saturated Sandstone Tuff: Exhibits resistivity values ranging from 14 to 70 Ωm.Breccia: Possesses resistivity values above 70 Ωm. The slip plane corresponds to the clay tuff, and its geometry aligns with the slope direction along tracks 1 and 2. The slip plane is found at a depth of approximately 10 meters. When the slope is unsaturated, meaning no water is retained within the landslide material, the calculated slope safety factor (SF) tracks 1 exceeds 1.25. This indicates that the unsaturated slopes are stable, resulting in a low likelihood of landslides. However, when the slope is saturated, the safety factor for track 1 below 1.07, indicating critical conditions and a higher risk of landslides.

References

[1] P. Arrogante-Funes, A. G. Bruzón, F. Arrogante-Funes, R. N. Ramos-Bernal, and R. Vázquez-Jiménez, "Integration of vulnerability and hazard factors for landslide risk assessment," *Int J Environ Res Public Health*, vol. 18, no. 22, Nov. 2021, doi: 10.3390/ijerph182211987.

[2] Z. Zakaria, I. Sophian, Z. S. Sabila, and L. H. Jihadi, "Slope Safety Factor and Its Relationship with Angle of Slope Gradient to Support Landslide Mitigation at Jatinangor Education Area, Sumedang, West Java, Indonesia," in *IOP Conference Series: Earth and Environmental Science*, Institute of Physics Publishing, May 2018. doi: 10.1088/1755-1315/145/1/012052.

[3] S. Xiao, W. Dong Guo, and J. Zeng, "Factor of Safety of Slope Stability from Deformation Energy." [Online]. Available: www.nrcresearchpress.com

[4] S. N. Nasution, S. Rachman, and H. Pramudito, "Slope stability analysis using bishop method and kinematic analysis," *IOP Conf Ser Mater Sci Eng*, vol. 1098, no. 6, p. 062041, Mar. 2021, doi: 10.1088/1757-899x/1098/6/062041.

[5] C. Prasetyadi *et al.*, "Conservation of groundwater in Nglanggran Area, Gunung Kidul District, Yogyakarta," in *IOP Conference Series: Earth and Environmental Science*, Institute of Physics Publishing, Dec. 2018. doi: 10.1088/1755-1315/212/1/012007.

[6] R. W. Van Bemmelen, *The Geology of Indonesia*, vol. IA. The Hague: U.S. Goverment Printing Office, 1949.

[7] Surono, "Litostratigrafi Pegunungan Selatan Bagian Timur Daerah Istimewa Yogyakarta Dan Jawa Tengah," *Jurnal Geologi dan Sumberdaya Mineral*, vol. 19, no. 3, pp. 209–221, 2009.

[8] L. P. Negara, D. Lestari, F. A. Kurnianto, F. A. Ikhsan, B. Apriyanto, and E. A. Nurdin, "An overview of depositional environment between the mountains of southern java and the fold mountain of north java," in *IOP Conference Series: Earth and Environmental Science*, IOP Publishing Ltd, Mar. 2021. doi: 10.1088/1755-1315/683/1/012005.

[9] B. Prastisho, P. Pratiknyo, A. Rodhi, and C. Prasetyadi, "03. Prociding SCIENE & TECHNOLOGY LPPM 2017 (1)," in *Prociding Science & Technlogy LPPM*, 2017, pp. 31–36.

[10] T. R. Rahmani, D. P. Sari, A. Akmam, H. Amir, and A. Putra, "Using the Schlumberger configuration resistivity geoelectric method to analyze the characteristics of slip surface at Solok," in *Journal of Physics: Conference Series*, Institute of Physics Publishing, May 2020. doi: 10.1088/1742-6596/1481/1/012030.

[11] A. Octova, A. S. Muji, M. Raeis, and R. R. Putra, "Identification of aquifer using geoelectrical resistivity method with schlumberger array in Koto Panjang Area, Nagari Tigo Jangko, Lintau Buo Sub-District, Tanah Datar Regency," in *Journal of Physics: Conference Series*, Institute of Physics Publishing, May 2019. doi: 10.1088/1742-6596/1185/1/012009.

[12] Y. Yatini and I. Suyanto, "Identification of slip surface based on geoelectrical dipole-dipole in the landslides hazardous area of Gedangsari District, Gunungkidul Regency, Province of Daerah Istimewa Yogyakarta, Indonesia," in *IOP Conference Series: Earth and Environmental Science*, Institute of Physics Publishing, Dec. 2018. doi: 10.1088/1755-1315/212/1/012013.

[13] E. Rolia and D. Sutjiningsih, "Application of geoelectric method for groundwater exploration from surface (A literature study)," in *AIP Conference Proceedings*, American Institute of Physics Inc., Jun. 2018. doi: 10.1063/1.5042874.

[14] O. R. Hermawan and D. P. Eka Putra, "The Effectiveness of Wenner-Schlumberger and Dipole-dipole Array of 2D Geoelectrical Survey to Detect The Occurring of Groundwater in the Gunung Kidul Karst Aquifer System, Yogyakarta, Indonesia," *Journal of Applied Geology*, vol. 1, no. 2, p. 71, Jul. 2016, doi: 10.22146/jag.26963.

[15] W. M. Telford, L. P. Geldart, and R. E. Sheriff, *Applied Geophysics*, Second. Cambridge: Cambridge University Press, 1990.

[16] A. W. Bishop, "First Technical Session : General Theory oj Stability of Slopes The Use Of The Slip Circle In The Stability Analysis Of Slopes," 1954.

[17] T. Zhang, Q. Cai, L. Han, J. Shu, and W. Zhou, "3D stability analysis method of concave slope based on the Bishop method," *Int J Min Sci Technol*, vol. 27, no. 2, pp. 365–370, Mar. 2017, doi: 10.1016/j.ijmst.2017.01.020.

[18] K. J. Agbelele, G. O. Adeoti, D. Y. Agossou, and G. G. Aïsse, "Study of Slope Stability Using the Bishop Slice Method: An Approach Combining Analytical and Numerical Analyses," *Open Journal of Applied Sciences*, vol. 13, no. 08, pp. 1446–1456, 2023, doi: 10.4236/ojapps.2023.138115.

[19] K. Gelisli, T. Kaya, and A. E. Babacan, "Assessing the factor of safety using an artificial neural network: case studies on landslides in Giresun, Turkey," *Environ Earth Sci*, vol. 73, no. 12, pp. 8639–8646, Jun. 2015, doi: 10.1007/s12665-015-4027-1.

[20] L. Li and X. Chu, "Failure Mechanism and Factor of Safety for Spatially Variable Undrained Soil Slope," *Advances in Civil Engineering*, vol. 2019, 2019, doi: 10.1155/2019/8575439.

[21] S. Mulyaningsih, M. Muchlis, N. W. A. A. T. Heriyadi, and D. Kiswiranti, "Volcanism in The Pre-Semilir Formation at Giriloyo Region; Allegedly as Source of Kebo-Butak Formation in the Western Southern Mountains," *Journal of Geoscience, Engineering, Environment, and Technology*, vol. 4, no. 3, p. 217, Sep. 2019, doi: 10.25299/jgeet.2019.4.3.2262.

[22] J. Castro, M. P. Asta, J. P. Galve, and J. M. Azañón, "Formation of clay-rich layers at the slip surface of slope instabilities: The role of groundwater," *Water (Switzerland)*, vol. 12, no. 9, Sep. 2020, doi: 10.3390/w12092639.

[23] R. Rekzyanti, S. Balamba, and L. Manaroinsong, "Analisa Kestabilan Lereng Akibat Gempa (Studi Kasus : Iain Manado)," vol. 14, no. 66, 2016.